

Chapter 8

Cooling of the Earth in the Archaean

8.1 Introduction

There is still considerable controversy over the mantle temperature during the Archaean (approx. 3.5-2.7 Gyr B.P.). On the one hand, high mantle temperatures are inferred from the occurrence of very magnesian komatiitic lavas, that are widespread in most Archaean greenstone belts, but rarely found after the Archaean-Proterozoic transition at 2.7 Gyr. These komatiites indicate high extrusion temperatures and melting temperatures some 400-500 K in excess of today's mantle temperatures. Some have taken this indicative of the average mantle temperatures [Sleep, 1979; Nisbet & Fowler, 1983; Vlaar, 1986]. Others assume the average mantle temperature to have been only 200-300 K higher than at present [Sleep & Windley, 1982; McKenzie, 1984; Jeanloz & Morris, 1986] and take the komatiite occurrence to be the consequence of hotspot activity. A third group proposes even lower temperatures for the Archaean [Campbell & Griffiths, 1992]. On the other hand, the temperatures at 50-100 km depth in the Archaean continents, as have been derived from high-grade terrains, indicate conditions that have not been very different from the present day situation. This 'Archaean paradox' has led many investigators to models in which cooling of the hotter Earth took place through rapid convection underneath the oceans. In most of these model studies it is implicitly assumed that mantle convection models can simulate present day plate tectonic processes, and that plate tectonics has been operative in the Archaean [e.g., Bickle, 1978; Davies, 1979; Schubert et al., 1980; Sleep & Windley, 1982]. However, the present day tectonic plate forces of 'slab pull' and 'ridge push' are strongly dependent on lithospheric age and hence on lithospheric recycling rate and mantle temperature. A uniformitarian extrapolation of present conditions to the Archaean may not be valid [Vlaar, 1985; 1986] and therefore, a different approach has to be adopted [Vlaar et al., 1993].

First, we will consider some previously published thermal cooling models of the Earth which have been used to constrain Archaean mantle temperatures. Next, the influence of higher temperatures on the pressure-release melting of mantle diapirs, and the related changes in upper mantle dynamics are considered. Finally,

we will present a model for the dynamics of the oceanic lithosphere and discuss its applicability to the cooling of the Earth in the Archaean.

8.2 Cooling models for the Earth based on parameterized convection

Several authors have studied thermal histories of the Earth using parameterized mantle convection models. In these, the change of average mantle temperature with time follows from the energy balance equation:

$$\frac{4\pi}{3} \rho c_p (R_m^3 - R_c^3) \frac{dT}{dt} = -4\pi q R_m^2 + \frac{4\pi}{3} Q (R_m^3 - R_c^3) \quad (8.1)$$

where q is the average heat flux out of the Earth's surface and Q is the average heat production in the mantle. The definition of the other parameters is given in table 8.1. The heat flux from the core into the base of the lower mantle is probably small [Stacey, 1977] and is neglected by most authors. For the mantle the Nusselt number Nu can be defined as the ratio of the total heat flux to the conductive heat flux out of the mantle

$$Nu = (q_{cond} + q_{conv})/q_{cond} = qD/k\Delta T \quad (8.2)$$

where ΔT is the temperature difference across the mantle. The relation between the Nusselt number and the vigour of convection in the mantle, which has been

Table 8.1 Notation and nominal values

Parameter	Definition	Value
g	gravitational acceleration	9.8 ms^{-2}
α	thermal expansivity	$3 \times 10^{-5} \text{ K}^{-1}$
κ	thermal diffusivity	$10^{-6} \text{ m}^2 \text{ s}^{-1}$
D	Depth of convection layer	$2.8 \times 10^6 \text{ m}$
ν	kinematic viscosity	
η	dynamic viscosity	
ν_0	Minimum kinematic viscosity	$2.21 \times 10^7 \text{ m}^2 \text{ s}^{-1}$
A	Activation temperature (γT_m)	$5.6 \times 10^4 \text{ K}$
k	thermal conductivity	$4.2 \text{ Wm}^{-1} \text{ K}^{-1}$
ρc_p	volumetric specific heat	$4.2 \times 10^6 \text{ Jm}^{-3} \text{ K}^{-1}$
R_c	core radius	$3.471 \times 10^6 \text{ m}$
R_m	mantle outer radius	$6.271 \times 10^6 \text{ m}$
Ra_c	critical Rayleigh number	1100
T_s	surface temperature	273 K
β	power law exponent	0.3

exploited in parameterized convection models, is

$$Nu = (Ra/Ra_c)^\beta \quad (8.3)$$

where Ra is the mantle Rayleigh number and Ra_c is the critical Rayleigh number, $Ra_c \sim 10^3$. For a mantle heated entirely from below Ra is defined by

$$Ra = Ra_E = \frac{\alpha g(T - T_S)D^3}{\kappa \nu} \quad (8.4)$$

This definition has been used by Sharpe & Peltier [1978] to study the loss of primordial heat, initially stored in the core, through mantle convection. For a mantle heated entirely from within Ra is defined by

$$Ra = Ra_I = \frac{\alpha g Q (R_m - R_c)^5}{\kappa^2 \nu \rho c} \quad (8.5)$$

In (8.1) the lower boundary of the mantle is explicitly assumed to be insulated, and the second definition of the Rayleigh number, Ra_I , should be used. However, Schubert et al. [1980], Jackson & Pollack [1984,1987] and McGovern & Schubert [1989] have used the first definition, based on the claim of Schubert et al. [1980] that this was justified if T in (8.4) represents the characteristic temperature of the convecting region.

A temperature-dependent rheology of the form

$$\nu = \nu_0 \exp(A/T) \quad (8.6)$$

has been used in the models. The parameter A can be interpreted as an activation temperature. Several formulations have been used to determine A , either using Weertman & Weertman's [1975] formulation based on homologous temperature ($A = \gamma T_m$, $\gamma \approx 30$), using activation energy ($A = E/R$), or both activation energy and volume ($A = (E + pV)/R$). Determination of the value of A , to be used in (8.6), from the formulations mentioned above is correct only for Newtonian fluids. In non-Newtonian fluids the activation temperature decreases with a factor n , an effect that has been neglected by several authors [e.g., Davies, 1979; Williams & Pan, 1992]. To include the effect of volatiles an effective A as a function of volatile content has been defined through the melting temperature T_m [Jackson & Pollack, 1987; Williams & Pan, 1992].

The general form of the heat production is

$$Q = Q_0 \exp(-\lambda t) \quad (8.7)$$

where λ is the decay rate of the radioactive material and Q_0 is the heat production at $t = 0$. Jackson & Pollack [1987] have used an effective λ to describe a mixture of several isotopes with different decay rates. Q_0 is not well known and in most calculations it has been used as a free parameter; Q_0 was varied to constrain the

present day heat flux at 70 mWm^{-2} , based on the estimate of oceanic heat loss [Sclater et al., 1980]. In contrast to this, Sleep [1979] and Stacey [1980] used the abundance of atmospheric ^{40}Ar to constrain absolute values of the concentration of ^{40}K and from that the concentrations of the other heat producing elements.

Substitution of (8.2)-(8.4), (8.6) and (8.7) into (8.1) gives

$$\frac{dT}{dt} = \frac{-3 \left[\frac{\alpha g (T - T_S) D^3}{Ra_c \kappa \nu_0 \exp(A/T)} \right]^\beta k (T - T_S) R_m^2}{D \rho c_p (R_m^3 - R_c^3)} + \frac{Q_0}{\rho c_p} \exp(-\lambda t) \quad (8.8)$$

This non-linear differential equation can be solved numerically. A typical result is shown in figure 8.1, that shows the averaged mantle temperature and mantle heat flow as a function of age. A fourth order Runge-Kutta scheme with a constant step size of 10 Myr has been used to solve (8.8). The nominal values shown in table 8.1 and a decay rate $\lambda = 4.48 \times 10^{-10} \text{ yr}^{-1}$ have been used. This decay rate corresponds to the time-averaged decay constant for a chondritic composition [Schubert et al., 1980]. The model run with $Q_0 = 220 \text{ nWm}^{-3}$ (bold line) yields a present day heat flow of 70 mWm^{-2} .

Other models include different distributions of radioactive heat sources [e.g.,

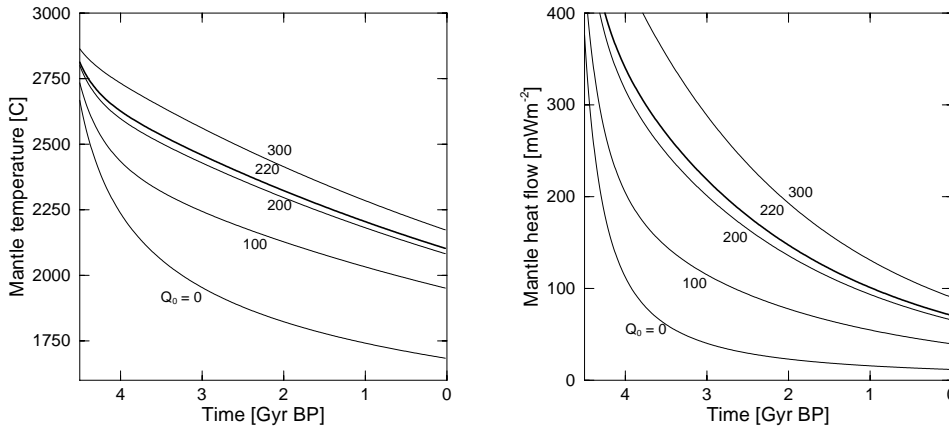


Figure 8.1 Example of evolution of internal mantle temperature and surface heat flow, based on parameterized mantle convection modelling (see text). Heat production is given by $Q(t) = Q_0 \exp(-\lambda t)$, where the decay constant $\lambda = 4.48 \cdot 10^{-10} \text{ yr}^{-1}$ is for a chondritic composition [Schubert et al., 1980]. The initial heat production Q_0 is used as a free parameter. $Q_0 = 220 \text{ nW} \cdot \text{m}^{-3}$ yields a present day heat flow of $70 \text{ mW} \cdot \text{m}^{-2}$.

Jackson & Pollack, 1984], volatile-dependent rheology and the de/regassing history of the Earth [McGovern & Schubert, 1989; Williams & Pan, 1992]. In general, the results show the strong self-regulating effect of the temperature- and volatile-dependent rheology on the dynamical cooling and a temperature decrease of 200-300 K since the Archaean. A lower estimate of the amount of cooling is made by Davies [1979], who derives from isoviscous models, that the Earth cannot have cooled by more than 100-150 K.

The assumptions and simplifications that have been used to make this analysis possible, make it difficult to judge the applicability of these models to the evolution of the Earth. One point of criticism applies to the employed Nusselt-Rayleigh number relationship, which in general does not take into account the effects of large aspect ratio convection [Hansen & Ebel, 1984], viscous dissipation [Steinbach, 1991], and depth variations in rheological [Hager, 1984] and thermodynamical properties [Chopelas et al., 1989; Osaka & Ito, 1991].

Another shortcoming of the models concerns the implementation of temperature-dependent rheology, as has been pointed out by Christensen [1984c; 1985]. He essentially indicates the importance of the rheology of the upper boundary layer in controlling the cooling of the Earth. As the surface temperature is assumed to have varied very little over geological times, the upper boundary layer may well have a rheology that is largely independent of the internal temperature. A consequence could be that the Nusselt number Nu would become independent of the Rayleigh number and heat flux would be constant throughout most of the Earth's history. As has been shown later, this effect might be less important for high Rayleigh number ($Ra > 10^8$) convection, for which the heat flow would become a function of Ra again, even for strongly temperature-dependent viscosity [U. Hansen, personal communication, 1993]. However, it is not clear if these high Rayleigh number convection results apply to the Earth, even in its early history.

In addition to this, Vlaar [1985; 1986] and Vlaar & Van den Berg [1991] have shown that the thicker basaltic and underlying depleted harzburgitic layer, that are created at higher mantle temperatures [e.g., Sleep, 1979], constitute a compositional boundary layer with a strong stabilizing influence, that might effectively prohibit plate tectonics in the way it operates today. This effect has been neglected thus far.

In order to study the thermal evolution of the Earth since the early Archaean, it is essential to incorporate these rheological and compositional properties of the upper thermal boundary layer. In present paper we will assume that the cooling of the Earth is completely governed by the dynamics of the upper boundary layer. Any sinking material is passively replaced by adiabatically upwelling mantle. This approach is similar to that of Sleep [1979], who used analytical half space cooling models, combined with estimates of the average age of the oceanic lithosphere, to study the thermal evolution.

8.3 Pressure-release melting

The process of pressure-release melting of undepleted mantle peridotite plays an important role in the Earth. It is held to be the cause of the present day generation of basaltic oceanic crust at mid-ocean ridges. It is generally agreed upon, that in a hotter mantle the melting of a rising diapir starts at a deeper level and a larger volume of basaltic magma is formed [e.g., Sleep, 1979; McKenzie, 1984; Vlaar, 1985; Takahashi, 1990]. McKenzie & Bickle [1988] derive the thickness of the formed basaltic crust as a function of the potential temperature of the mantle, which is the absolute mantle temperature extrapolated along the adiabat to zero pressure. Estimates for the present day potential temperature range from 1280 °C to 1400 °C [Sleep, 1979; McKenzie, 1984; Christensen, 1985; Abbott et al., 1993]. The range indicates the uncertainties in eruption temperatures of basaltic magmas and in the temperature drop as a consequence of the latent heat consumption. An important effect that has not been implemented by McKenzie & Bickle [1988], is that the amount of melting will be influenced by the pressure that is exerted by the already formed basaltic crust. This will lead to considerably less production of basaltic crust upon pressure-release melting [Vlaar & Van den Berg, 1991].

Figure 8.2a illustrates the effect of higher mantle temperature on the melting of an adiabatically rising diapir, using the formalism developed by McKenzie [1984], corrected for the crustal pressure effect [Vlaar & Van den Berg, 1991]. Shown are the solidus and liquidus of mantle peridotite, each given as a third order polynomial fit to the data of Takahashi [1990], $T(p) = a_0 + a_1 p^1 + a_2 p^2 + a_3 p^3$. The coefficients can be written as a vector \mathbf{a} . These are given, with pressure in Gpa and temperature in °C, by $\mathbf{a} = (1136, 134.2, -6.581, 0.1054)^T$ for the solidus, and $\mathbf{a} = (1762, 57.46, -3.487, 0.0769)^T$ for the liquidus. The dotted lines indicate lines of equal melting for 15 and 50 % melting, based on data from Jaques & Green [1980]. For the entropy of melting we used $\Delta S = 300 \text{ J} \cdot \text{kg}^{-1} \text{K}^{-1}$, which is approximately equivalent to $1 R \text{ J} \cdot \text{mol}(\text{atom})^{-1} \text{K}^{-1}$ [Jeanloz, 1985; Miller et al., 1991]. The bold lines indicate the (T,p)-paths for rising diapirs at three different potential temperatures, $T_{pot} = 1330, 1600, \text{ and } 1750 \text{ }^\circ\text{C}$. The present day situation, with a crustal thickness of 7 km, is simulated with $T_{pot} = 1330 \text{ }^\circ\text{C}$. The extrusion temperature here is $T_{extr} = 1240 \text{ }^\circ\text{C}$. At $T_{pot} = 1600 \text{ }^\circ\text{C}$, 29 km of basaltic crust is generated with $T_{extr} = 1420 \text{ }^\circ\text{C}$. At the highest potential temperature shown, $T_{pot} = 1750 \text{ }^\circ\text{C}$, melting of a rising diapir generates 50 km of basaltic crust with $T_{extr} = 1520 \text{ }^\circ\text{C}$. Note the strong effect of the consumption of latent heat on the extrusion temperatures. Although the potential temperatures differ by 420 °C, the temperatures at 50 km depth differ only by 280 °C.

Figure 8.2b shows the density in the underlying depleted harzburgitic residue for the three cases with different potential temperature. The density of the

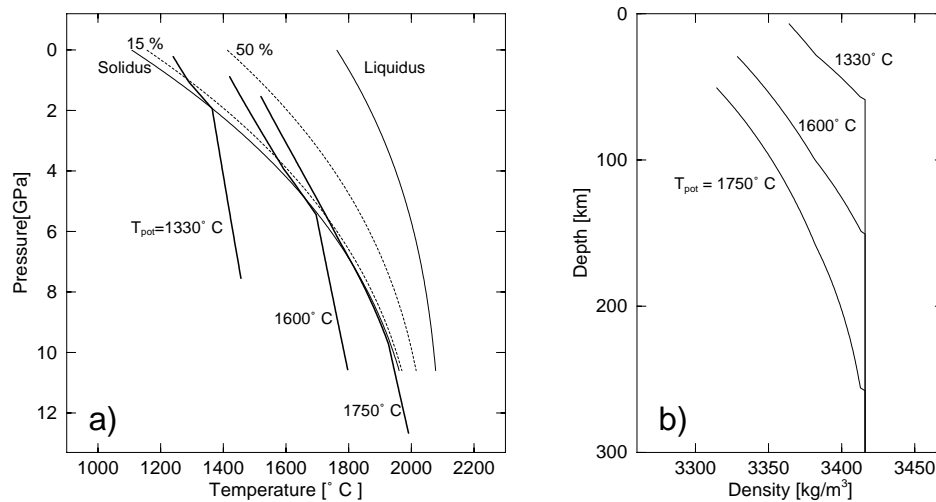


Figure 8.2 a) The effect on higher mantle temperatures on the pressure-release melting of a adiabatically rising diapir. The solidus and liquidus of mantle peridotite are shown as a third order polynomial fit (see text). Lines of equal melting for melt fraction 15 % and 50 % are shown, based on data by Jaques & Green [1980]. The thick solid lines indicate schematically the (T,p) -paths of a rising diapir at potential temperatures $T_{pot} = 1330$, 1600, and 1750 °C, based on McKenzie [1984]. In the calculations we have corrected for the crustal pressure effect [Vlaar & Van den Berg, 1991] (see text).

b) Compositional density in harzburgite and lherzolite. Density increases with depth, as a consequence of the lower degree of depletion.

harzburgite increases with depth as a consequence of the decreasing amount of depletion. As has been shown by Vlaar [1985] and Vlaar & Van den Berg [1991], this compositional stratification has a large effect on the stability of the oceanic lithosphere.

In this scenario, komatiite might be the melt generated at considerable depth (>150 km) and low degrees of partial melting. At depth, the komatiitic magma separates from the matrix and rises adiabatically to the surface [O'Hara, 1975; McKenzie, 1984; Takahashi, 1990]. This can explain the occurrence of komatiites as the first extrusion product in greenstone belt formation, followed by outflows of less MgO-rich basaltic lavas [Nisbet, 1987].

In the following section we will discuss the consequences of this for the dynamics of the lithosphere in a hotter mantle.

8.4 Consequences for upper mantle dynamics

Vlaar [1985; 1986] presented qualitative constraints on Archaean global dynamics, which are summarized by the following:

i) The mantle was originally molten, shortly after accretion [e.g., Stevenson, 1989].
ii) Rapid solidification started at the bottom of the mantle and progressed upward [Miller et al., 1991], until the whole mantle was at or below the solidus temperature.
iii) At high mantle temperatures, pressure-release melting of rising diapirs generates a thick basaltic layer on top of a very thick harzburgitic layer [Sleep, 1979; Vlaar, 1985; McKenzie & Bickle, 1988].
iv) Compositional stability [Vlaar, 1975; Vlaar & Wortel, 1976; Oxburgh & Parmentier, 1977] and lack of mechanical coherency of this upper boundary layer [Hoffman & Ranalli, 1988], renders modern style plate tectonics ineffective [Vlaar, 1985; 1986].
v) Continents stabilized on top of strong chemical zonation in harzburgitic root and the generation of radiogenic heat in the continental crust blankets the surface cooling [Vlaar, 1985].
vi) After formation of stable basalt-harzburgite layering, recycling of basaltic material can occur through its denser phases garnet-granulite and eclogite. The recycling of eclogite allows for new generation of basaltic magma.

In the following section we will consider the consequences of these constraints on the evolution of the lithosphere and upper mantle in a hotter Earth.

8.5 Dynamical modelling

Model description

We have employed a 2-dimensional thermochemical model of the cooling of the lithosphere and upper mantle (to 400 km depth), both in an oceanic and continental setting, schematically indicated in figure 8.3. In the continental model (figure 8.3a) a crust of 40 km thickness (consisting of a 10 km thick granitic upper crust on top of a 30 km thick more tonalitic or granulitic lower crust) overlies a thick harzburgitic root. The radioactive heat production is indicated in figure 8.3a. The value of the upper crust is based on the estimate for the heat production of a surface shield [O'Connell & Hager, 1980], corrected for the assumed three times higher productivity in the early Earth. The lower crust is assumed to have a 10× lower heat production. The oceanic lithosphere/upper mantle (figure 8.3b) comprises the layering formed through decompression melting of rising diapirs, with basalt (B) on top of depleted peridotite (harzburgite; Hz), overlying the undepleted mantle peridotite (lherzolite; Lh). The harzburgite layer has a density gradient as a consequence of the varying degree of depletion by partial melting with depth. The properties of the layering are strongly dependent on potential mantle temperature.

The stability of these models against cooling from the top is considered. The

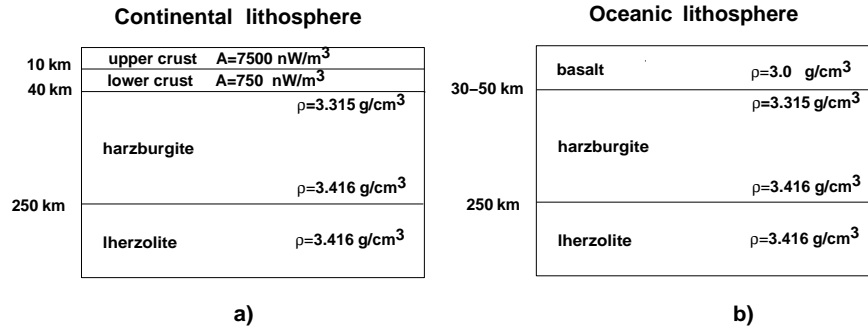


Figure 8.3 Schematic overview of the compositional layering for the a) continental and b) oceanic lithosphere-upper mantle in a 'hot Earth', with potential temperatures $T_{pot} > 1600$ °C.

free-slip upper boundary is kept at constant temperature $T = 0$ °C. At the lower boundary a constant, adiabatic temperature gradient is maintained.

To describe the rheology of the lithosphere and mantle, we have used linearized ductile creep laws, following Hoffman & Ranalli [1988]. The general form of the creep law is given by

$$\sigma = (\dot{\epsilon}/A)^{1/n} \exp(E/nRT) \quad (8.9)$$

where σ is differential stress (in MPa), $\dot{\epsilon}$ the strain rate (in s^{-1}), n the power law index, E the activation energy (in $Jmol^{-1}K^{-1}$), R the gas constant ($8.314 Jmol^{-1}$), T the absolute temperature (in K). Note that σ here is specified in MPa. From this we can derive an effective viscosity $\eta = \sigma/2\dot{\epsilon}$ (MPa · s), which can be expressed as

$$\eta = C \exp(E/nRT) \quad (8.10)$$

where

$$C = \frac{10^6}{2} \cdot \left[\frac{\dot{\epsilon}^{1-n}}{A} \right]^{1/n} \quad (\text{Pa} \cdot \text{s}) \quad (8.11)$$

The numerical values for diabase have been used to model basalt and eclogite, the values for peridotite have been used to model harzburgite and lherzolite. Tabel 8.2 gives the values for A , n and E from Hoffman & Ranalli [1988] and the value of C for $\dot{\epsilon} = 10^{-15} s^{-1}$. Figure 8.4 shows the effective viscosity of diabase and peridotite as a function of temperature.

The equations governing the models are the Stokes equation together with the

Table 8.2 Parameters used in the rheological description (8.11)

Rock	$\log A$ ($\text{MPa}^{-n}\text{s}^{-1}$)	n	E (kJmol^{-1})	C ($\text{Pa} \cdot \text{s}$)
Diabase	-2.5	3.3	268	81×10^{15}
Peridotite	4.5	3.6	535	19×10^{14}

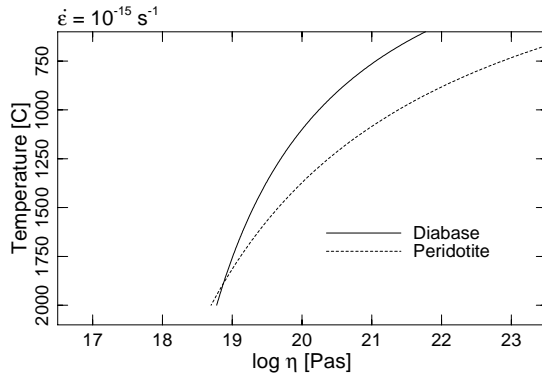


Figure 8.4 Effective viscosity of diabase (used to model basalt and eclogite) and peridotite (used to model harzburgite and lherzolite) as a function of temperature. Rheological parameters are defined in table 8.2.

incompressibility constraint, the advection-diffusion equation for temperature and the advection equation for the composition, as have been derived in Chapter 2. The equations are solved numerically by finite element methods. The Stokes equation is solved in the stream function formulation (2.22), using the non-conforming element (refer chapter 3). The time-dependent heat equation (2.3) is solved using linear triangles and a predictor-corrector method. The Boussinesq approximation is used and the adiabatic temperature increase with depth has no influence on the dynamics of the model. In the numerical model this adiabatic temperature is subtracted from the absolute temperature. The absolute temperature is used in the calculation of viscosity and for output purposes. For the advection equation for the composition we have used a mixed approach. The discontinuous density jumps, as e.g. between the basalt and harzburgite (figure 8.2b) are modelled using a marker-chain method. The density gradient in the harzburgite is modelled using a field approach. In this an explicit solution of the hyperbolic equation (2.4) is required. The time step in the predictor-corrector method was taken as 50 % of the Courant time step (refer chapter 3), with an upper limit of 1 Myr.

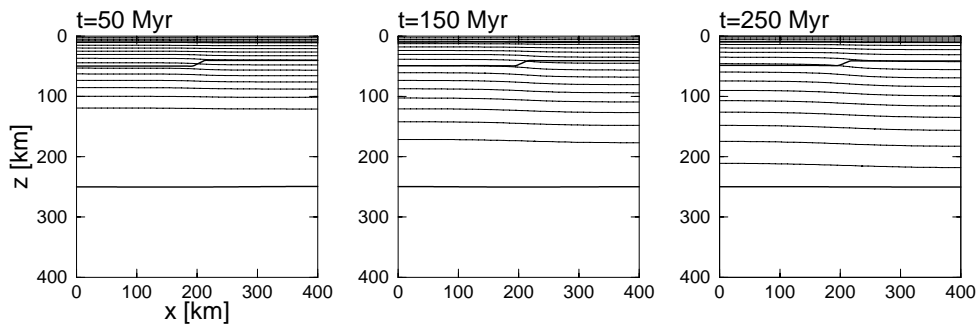


Figure 8.5 Evolution of a cooling continental lithosphere. The compositional stratification and distribution of heat producing elements are defined in figure 8.3. Retarded by the crustal heat production, the cooling progresses slowly to deeper levels. As a consequence of the density gradient in the harzburgitic root, the lithosphere remains stably stratified.

Results

Continental lithosphere, potential temperature 1750 °C

The evolution of the continental lithosphere is shown in figure 8.5. The lower crust is slightly thicker on one side of the model, to avoid that the model remains artificially stably stratified. The first frame shows the initial temperature profile, based on the (T,p)-path of a rising diapir. The crustal heat production balances ("blankets") only partially the heat loss through the top and the cooling progresses slowly to larger depths. As is shown in figure 8.5, the continental lithosphere is stable to at least 250 Myr. After this, the cooling progresses into the undepleted peridotitic layer. In some simulations this creates an instability in the lower parts of the model, which can recycle the lowermost parts of the (now thermally defined) continental root. However, the most important result of these simulations is that the proposed layering is intrinsically stable to cooling. This leads to a firm basis of the suggestion that the early proto-continents have been able to resist recycling on top of a chemically zoned root, and that the present thickness of the continental cratons (~ 200 km) has been maintained throughout geological history.

Oceanic lithosphere, potential temperature 1750 °C

The oceanic lithosphere, formed at $T_{pot} = 1750$ °C, is stably stratified in a similar fashion as the continental lithosphere, discussed above. Recycling of the basaltic crust and underlying harzburgite can only be achieved in this environment through the formation of the denser phases of gabbroic basalt: viz., garnet-granulite (GG;

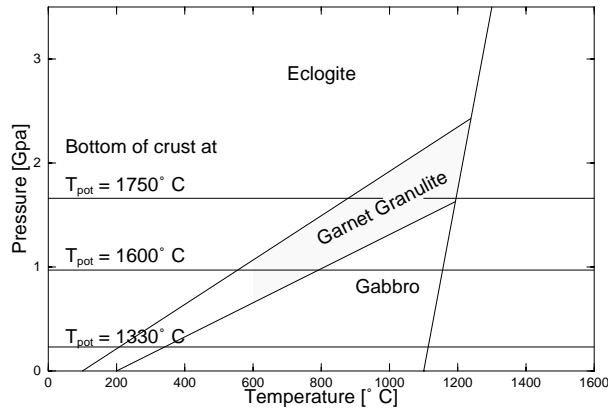


Figure 8.6 Phase diagram for basalt [after Ringwood, 1975].

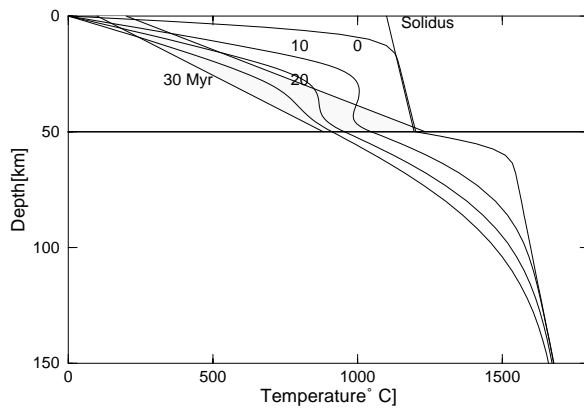


Figure 8.7 Evolution of the horizontally averaged temperature in the oceanic lithosphere, generated at $T = 1750$ °C. Convection in the basalt generates an asthenosphere and relatively cool temperatures in the lower crust.

$\rho \sim 3.3 \text{ g} \cdot \text{cm}^{-3}$) and eclogite (E; $\rho \sim 3.6 \text{ g} \cdot \text{cm}^{-3}$). Figure 8.6 shows a phase diagram for basalt, taken from Ringwood [1975]. The horizontal lines indicate the pressures at the base of the crust, formed at $T_{pot} = 1750$, 1600 and 1330 °C, resp. At $T_{pot} = 1750$ °C, the crust is approximately 50 km thick and solid state convection can occur in the basaltic layer (assuming that the upper brittle crust has negligible influence on the dynamics). Figure 8.7 shows the evolution of the horizontally averaged temperature in the oceanic lithosphere. The initial temperature

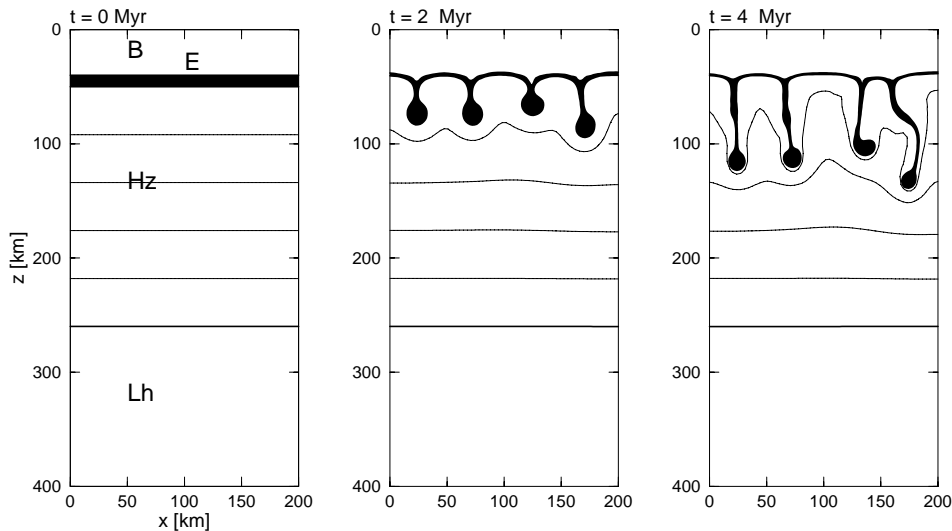


Figure 8.8 The recycling of eclogite into the upper mantle. Original oceanic lithosphere generated at $1750\text{ }^{\circ}\text{C}$.

profile underneath the basalt layer is taken from figure 8.2a. It is assumed that, after formation the basaltic crust solidified very rapidly and that the basalt is at its solidus temperature, except for the thin boundary layer on top. The grey area indicates the garnet-granulite stability field, taken from figure 8.6. Cooling progresses rapidly through the efficient heat loss by the combined effects of conduction and low Rayleigh number convection. After 10 Myr, the lower part of the crust is in the garnet-granulite stability field. Garnet-granulite is nearly as dense as the underlying harzburgite. The cooler garnet-granulite may have sufficiently high density to recycle into the mantle, although the density difference with the underlying harzburgite is not very large. A more efficient way of recycling the basaltic crust is through its high density phase eclogite. This is considered in the following paragraphs.

When it is just formed, the brittle layer is thin and weak [Hoffman & Ranalli, 1988], and can probably not resist sinking into the hot ductile lower crust. Through this mechanism of crustal or 'mini'-subduction, a relatively cool ($T < 1000\text{ }^{\circ}\text{C}$) and hydrated basaltic layer can be formed on top of the harzburgite. Under these conditions, the transformation from gabbro to eclogite is fast, with time scales on the order of 1 Myr [Ahrens & Schubert, 1975]. Once eclogite is formed, recycling of crustal material into the harzburgitic layer is fast. Figure 8.8 illustrates this for a layering formed at potential temperature $T_{pot} = 1750\text{ }^{\circ}\text{C}$. The eclogite layer has a thickness of 10 km. Within 5 Myr most of the eclogite is recycled into the

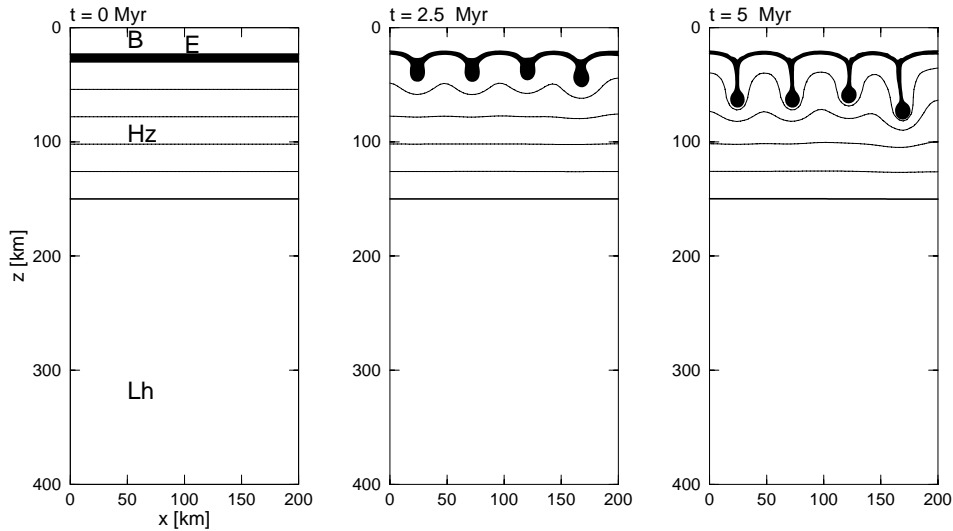


Figure 8.9 The recycling of eclogite into the upper mantle. Original oceanic lithosphere generated at $1600\text{ }^{\circ}\text{C}$.

underlying harzburgite. The harzburgite wells up passively and, if the top of the harzburgite is still hot enough, new basalt can be formed by pressure-release melting.

We propose that this mechanism of recycling of basaltic crust through mini-subduction, rapid eclogitization at the bottom of the crust, recycling of the eclogite into the upper mantle and formation of new crust by pressure-release melting, is responsible for the initial cooling of the hot Earth, after solidification of the mantle.

Oceanic lithosphere, potential temperature $1600\text{ }^{\circ}\text{C}$

At lower potential temperature, the proposed mechanism of cooling of the Earth will become less efficient, and eventually cease to occur. The viscosity of the lower basaltic crust and harzburgite increases, the recycling of hydrated crust will become less efficient and eclogitization is less rapid. The less efficient eclogitization of the lower crust is the main factor determining the lower speed of the mechanism. The increase in viscosity and thinning of the eclogite layer have only a minor effect, as is illustrated in figure 8.9, where the recycling of a now 5 km thick eclogitic layer is shown in a model based on a basalt-harzburgite layering formed at $T_{pot} = 1600\text{ }^{\circ}\text{C}$. The basaltic crust has a total thickness of 29 km. Initial temperature and compositional density are given for the harzburgite/lherzolite in figures

8.2a-b. Recycling of the eclogite layer is now approximately $2\times$ slower.

At even lower temperatures, the crust will become too thin and the brittle upper crust too strong for crustal subduction to take place and pressures at the bottom of the crust may be too low for eclogite to be formed, although it is not clear at which crustal thickness this will occur. The phase diagram for basalt (figure 8.6) indicates that eclogite cannot be formed at crustal thicknesses below ~ 25 km. However, some evidence exist for the formation of eclogite from hydrated basalt at shallower levels [Ahrens & Schubert, 1975]. The driving forces of the present day form of plate tectonics will become increasingly important and in a certain temperature range a gradual transition from the proposed mechanism and plate tectonics may occur. Tentatively, we put this transition at a potential "blocking" temperature of $T_{pot} = T_0 = 1475$ °C, at which 15 km of crust is produced.

8.6 A thermal model for the early Earth

We will now turn to the consequences of the presented dynamical model for the thermal history of the Earth. Our approach to this problem is necessarily speculative, due to the lack of detailed knowledge on the interaction between the different processes and the variability of the parameters governing the dynamical behaviour.

We assume that the cooling of the Earth's mantle is entirely caused by heat loss through the oceanic lithosphere. At present, this is estimated at 3×10^{13} W, predominantly (> 90 %) by the conductive cooling of the continuously recycling lithosphere [Sclater et al., 1980]. The consumption of latent heat at mid-oceanic ridges is only a fraction of this [Takahashi, 1990]. However, in a hotter mantle, the amount of melt generated is much larger and the dissipation of heat by magma generation may be the dominant form of cooling of the Earth [Ogawa, 1988; Takahashi, 1990]. We will use this and estimate the amount of cooling in our models by i) consumption of latent heat by pressure-release melting, ii) advection of magma to the surface, and iii) conductive cooling of the basaltic crust. Key parameter in this is the rate of recycling of basaltic crust through the eclogite phase. We will make some simplifying assumptions regarding the recycling process. Consider the 1-D lithospheric column depicted in figure 8.10a. Removal of the eclogitic layer will result in passive upwelling of the total column underneath the crust, leading to renewed pressure-release melting. The amount of latent heat consumed upon melting is equal to $\rho L \dot{V}$, where $\rho = 3000 \text{ kg} \cdot \text{m}^{-3}$ is the density, $L = 6 \times 10^5 \text{ Jkg}^{-1}$ the latent heat of basalt melt [Fukuyama, 1985], and \dot{V} the rate of eclogite recycling (in $\text{m}^3 \cdot \text{s}^{-1}$). The basaltic magma is generated at a specific extrusion temperature T_{extr} . Percolation of magma to the surface will continue until the temperature in the basaltic layer is below the solidus temperature, leading to additional heat loss,

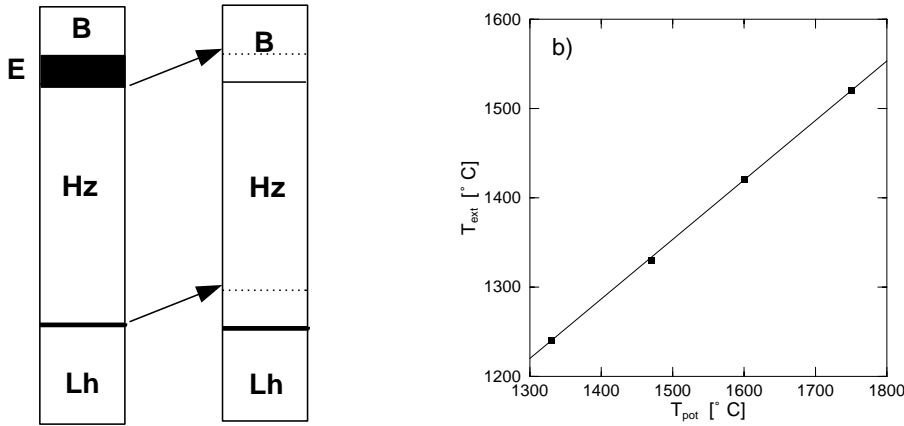


Figure 8.10 a) Cooling of a lithospheric column through pressure-release melting. Recycling of the eclogitic layer leads to uplift of the entire column below the crust and heat loss by consumption of latent heat and magma migration. b) Dependence of extrusion temperature T_{extr} on the potential temperature T_{pot} . Points indicate the calculations made using the formalism of McKenzie [1984], corrected for the crustal pressure effect [Vlaar & Van den Berg, 1991]. The solid line indicates the first order approximation $T_{extr} = 2/3 \times (T_{pot} - 1330) + 1240$ °C.

estimated at $\rho c_p \dot{V}(T_{extr} - T_{SB})$, where $c_p = 1.3 \times 10^3 \text{ Jkg}^{-1}\text{K}^{-1}$ is the specific heat and $T_{SB} = 1200$ °C the solidus temperature of basalt (assumed constant here). Furthermore, we will assume that the process of eclogite recycling is continuous and that this process leads to a continuous decrease in mantle temperature. The amount of crustal recycling is strongly dependent on potential temperature, through the processes describe above. We will parameterize this influence as a linear function $\dot{V} = a(T_{pot} - T_0)$. The parameter a depends on the rates of crustal subduction, eclogite formation and eclogite recycling. In the 1-D column the maximum combined rate is determined by the recycling rate of eclogite, which can be estimated from the results above to be $\sim 5 \text{ km} \cdot \text{Myr}^{-1}$ at $T_{pot} = 1750$ °C. Assuming that 70 % of the Earth's surface is oceanic, we can convert this to an effective rate

$$\dot{V}_{max} = (5 \text{ km} \cdot \text{Myr}^{-1}) \times (0.7 \times 5 \times 10^8 \text{ km}^2) = 1.8 \times 10^9 \text{ km}^3 \text{Myr}^{-1} \quad (8.12a)$$

with corresponding

$$a_{max} = 6.4 \times 10^6 \text{ km}^3 \text{Myr}^{-1} \text{K}^{-1} \quad (8.12b)$$

The extrusion temperature T_{extr} depends on the potential temperature as well. In a first order approximation this dependence is given by (figure 8.10b):

$$T_{extr} = 2/3 \times (T_{pot} - 1330) + 1240 \text{ }^\circ\text{C} \quad (8.13)$$

In this model, we can only guess at the rate of cooling through conductive heat loss. The dynamic models presented above indicate only the efficiency of eclogite recycling, once it is formed. It does not provide us with information on the processes controlling melt segregation, melt migration and the temperature distribution in the lithospheric column as has been described above. We estimate that, in comparison to the heat loss by latent heat consumption and melt migration, conductive cooling has only a minor contribution to the total heat loss in the hotter Earth. For practical purposes, we assume that the conductive heat loss has not varied throughout geological time, and fix it at the present day value of

$$4\pi q R_m^2 = 3 \times 10^{13} \text{ W} \quad (8.14a)$$

In comparison, at the highest estimated recycling rate \dot{V}_{\max} , the cooling through latent heat consumption contributes

$$\rho L \dot{V}_{\max} = 2 \times 10^{14} \text{ W} \quad (8.14b)$$

and the melt migration contributes ($T_{pot} = 1750 \text{ }^\circ\text{C}$)

$$\rho c_p (T_{extr} - T_{SB}) \dot{V}_{\max} = 1.5 \times 10^{14} \text{ W} \quad (8.14c)$$

We can now model the thermal evolution of the Earth using an extension to (8.1), given

$$\begin{aligned} \frac{4\pi}{3} \rho c_p (R_m^3 - R_c^3) \frac{dT}{dt} = & -4\pi q R_m^2 + \frac{4\pi}{3} Q (R_m^3 - R_c^3) \\ & - \rho c_p \dot{V} (T_{extr} - T_{SB}) - \rho L \dot{V} \end{aligned} \quad (8.15)$$

The temperature T is the mean mantle temperature, which is assumed to be the temperature at 1500 km depth. The relation with the potential temperature is given $T = T_{pot} + 750$, assuming a constant adiabatic gradient of $0.5 \text{ K} \cdot \text{km}^{-1}$. Heat production Q is modelled using Sleep's [1979] estimates of the absolute abundance of K, U and Th from the amount of ^{40}Ar . Figure 8.11 shows the evolution of the model, initially with $T_{pot} = 1750 \text{ }^\circ\text{C}$, for initial crustal recycling rates $\frac{1}{2} \dot{V}_{\max}$, $\frac{1}{5} \dot{V}_{\max}$, and $\frac{1}{10} \dot{V}_{\max}$, resp. Shown are from left to right the potential temperature T_{pot} (in $^\circ\text{C}$), latent heat consumption and heat advected by migrating melt (both in 10^{12} W). At potential temperature $T_0 = 1475 \text{ }^\circ\text{C}$, it is assumed that the mechanism becomes inefficient and heat loss is governed by conductive heat loss (8.14a) only. At the highest recycling rate shown the Earth cools by more than 200 K within 200 Myr. At $t = 0.5 \text{ Gyr}$, the blocking temperature T_0 is reached. At the lower recycling rates the cooling progresses slower, but still a large drop in temperature is observed in 1 Gyr. These results should be considered with proper caution as they

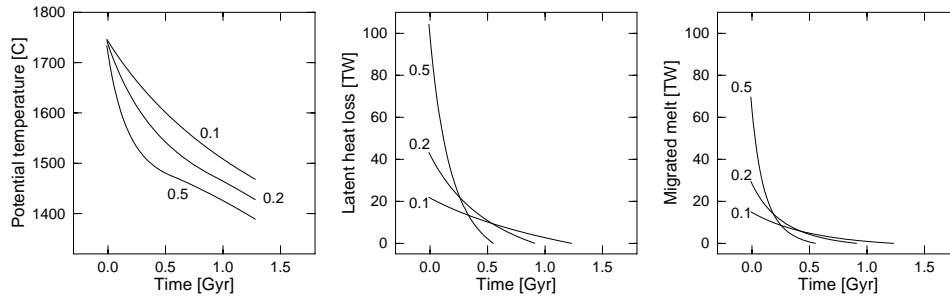


Figure 8.11 Influence of the latent heat loss and melt migration on the internal temperature of the Earth (8.15). Numbers indicate the crustal recycling rate at the arbitrary starting point, put at $t = 0$, relative to the proposed maximum \dot{V}_{\max} (8.12a).

are based on a rather speculative quantification and error margins are large. Most likely the conductive heat loss has been larger than modelled here, leading to a more efficient cooling. The estimates for the radiogenic heat production of Sleep [1979] are rather low compared to others. Increasing the heat production by a factor of two leads to much longer cooling times. However, it is not fully unreasonable to assume that, when the proposed mechanism has been active at some time in the Earth's history, it has efficiently cooled the mantle by several hundreds of degrees in, say, a 500 Myr period, leading to a moderate mantle temperature, maybe some 100-200 K higher than the present day situation.

Geological constraints on the thermal development of the upper mantle are given by the extrusion temperatures of volcanic rocks. Komatiites indicate the highest mantle temperatures, approx. $T_{pot} = 1650 - 1750^{\circ}\text{C}$ at 3.5 Gyr B.P., and $T_{pot} = 1500 - 1600^{\circ}\text{C}$ at 2.7 Gyr B.P. These are based on the estimates of the extrusion temperatures of the komatiites [e.g., Arndt & Nesbit, 1982] and the *ad hoc* estimates of the amount of latent heat, necessary to generate komatiitic melt at depth, ranging from 0°C [McKenzie, 1984; Takahashi, 1990] to 100°C [Sleep, 1979]. Other Archaean volcanic rocks, like ophiolites and greenstones, have extrusion temperatures that are distinctly lower. Abbott et al., [1993] determine for these rocks, that the mean extrusion temperature has decreased by approximately 150 K since the early Archaean (3.5 Gyr B.P.). Assuming that they are generated by pressure-release melting, a decrease in potential mantle temperature of 250 K can be inferred. It is not unreasonable to assume that the mean Archaean mantle temperature has been some 200-300 K higher than present day's. Even higher mantle temperatures imply conditions that are more favourable for eclogite formation and recycling as a consequence of the thicker basaltic layer, lack of mechanical coherency and larger mobility of the crust and upper mantle. The remelting of

eclogite upon recycling at moderate depths (50-100 km; see figure 8.7) may well have been important in the formation of tonalitic proto-continent in the very early Archaean [Condie, 1984]. The middle to late Archaean could have been characterized by some form of 'flake tectonics' [Hofmann & Ranalli, 1988], at the transition between the hot Earth dynamics and the present day plate tectonics. At these moderately higher upper mantle temperatures, the basaltic crust is still thick enough to resist lithospheric subduction, but is probably thin enough to allow for efficient eclogite formation and recycling.

8.7 Discussion

In the above, we have illustrated, quantitatively, some dynamical effects that can occur in a hotter mantle. Using the results of the dynamical modelling, we can envisage a strong episodic behaviour of the upper boundary layer, with periods of relative stabilization and conductive cooling followed by strong magmatic activity as a consequence of the thermal and compositional instability of the lower basaltic crust.

The interaction between the different mechanisms has yet to be explored. Presently, this is hampered by technical difficulties: a high resolution both in time and space is necessary to resolve the complex interaction. A large problem is presented by the different time scales at which relevant processes take place, as for example the migration of magma compared to the deformation of the solid phase. Studying one of these processes necessitates simplifying assumptions of the other one, although the two processes are dependent on each other.

Comments on rheological parameters

The rate of recycling is strongly dependent on the rheology of the basalt/eclogite and harzburgite. Some field evidence exists that eclogite has a lower viscosity than basalt [Austrheim, 1991]. We have taken this into account in some model calculations but no large difference was observed: as harzburgite is more viscous than both basalt and eclogite at the ambient temperatures (figure 8.4), it controls the speed of the sinking eclogite. In some models we have included pressure-dependence by extending the Arrhenius term in (8.9): $\sigma \sim \exp[(E + pV)/nRT]$, where p is the pressure and V the activation volume, which was assumed constant, $V = 10 \text{ cm}^3 \text{ mol}^{-1}$. The pressure-dependence is relatively unimportant in the upper 100 km and, consequently, little influence on the dynamics could be observed. The linearization of the power law creep law (8.9) will not be correct for strain rates much higher or lower than $\dot{\epsilon} = 10^{-15} \text{ s}^{-1}$. In the highest temperature models the recycling of eclogite

ite took place at strain rates significantly higher than this. The non-Newtonian effects will help drain the eclogitic layer even faster.

Venus

It is interesting to note a similarity of the presented models, with one that has recently been proposed for Venus by Parmentier & Hess [1992]. These authors studied the influence of the chemical stability of the lithosphere on the dynamics of Venus. They found that by surface cooling the Venusian lithosphere would become periodically unstable (with a characteristic period of 300-500 Myr) and resurfacing of Venus would occur. This model has been used to explain the relatively young crust (with ages of at most 500 Myr), as has been inferred from the record of impact cratering [Solomon, 1993]. The time scales found by Parmentier & Hess [1992] are much longer than we find in present paper. The efficient recycling and eclogitization of the hydrated upper crust as is proposed for the 'hot Earth' is not likely to work on Venus, as a consequence of the absence of water. Delamination of the upper and lower basaltic crust and consequent recycling of the cold and brittle upper crust is much less efficient. Moreover, the reaction time of the dry gabbro-eclogite transition is very long: probably on the order of 100 Myr [Ahrens & Schubert, 1975].

Coupling between upper and lower mantle

In the model presented above, we assumed that the cooling of the Earth is completely governed by the dynamics of the upper boundary layer and that any sinking material is replaced by passively upwelling mantle material. This is probably too simple a viewpoint, considering the mounting evidence for the strong influence of the transition zone on mantle dynamics. In recent modelling it has been shown that the thermodynamical [e.g., Christensen & Yuen, 1984; Machetel & Yuen, 1989; Steinbach & Yuen, 1992], compositional [Kellogg, 1991; Hansen et al., 1993] and rheological [Van Keken et al., 1992] properties of the transition zone will retard the exchange of material between upper and lower mantle. One can think of a scenario in which the upper mantle is efficiently cooled on top of a temporarily insulated lower mantle, until the temperature difference between upper and lower mantle is sufficiently large to overcome the resistance of the transition zone and large parts of the cold upper mantle are replaced by hot lower mantle. This mechanism may have occurred periodically through geologic time. The occurrence in the mid-Cretaceous of a sudden increase in plate velocities and crustal formation, combined with the eruption of massive flood basalts [Larson, 1991], may be understood in this way, and the abundant occurrence of komatiites in the Archaean may well have been a consequence of the episodic mixing between upper and lower mantle.

8.8 Conclusions

We have investigated some aspects of the dynamical behaviour of a proposed mechanism to cool the Earth in the Archaean. This mechanism involves thermal and compositional advection in a strongly stratified oceanic lithosphere at high average mantle temperatures. The basaltic crust is recycled into the mantle through its high pressure phase eclogite, leading to renewed pressure-release melting and basaltic crust formation. Consumption of latent heat and the advective cooling through magma migration is sufficient to cool the mantle in the (early) Archaean by several hundreds of degrees.

Acknowledgements

David Yuen, Ulli Hansen and Tanja Zegers are thanked for stimulating discussions. Wim Spakman is gratefully acknowledged for providing his graphical software.